PHYSICAL REVIEW B **91**, 140407(R) (2015)

Spin Hamiltonian, order out of a Coulomb phase, and pseudocriticality in the frustrated pyrochlore Heisenberg antiferromagnet FeF_3

Azam Sadeghi,[1] Mojtaba Alaei,[1,*] Farhad Shahbazi,[1,†] and Michel J. P. Gingras[2,3,4,‡]

[1]*Department of Physics, Isfahan University of Technology, Isfahan 84156-83111, Iran*
[2]*Department of Physics and Astronomy, University of Waterloo, Waterloo, Ontario N2L 3G1, Canada*
[3]*Perimeter Institute for Theoretical Physics, 31 Caroline North, Waterloo, Ontario N2L 2Y5, Canada*
[4]*Canadian Institute for Advanced Research, 180 Dundas Street West, Suite 1400, Toronto, Ontario M5G 1Z8, Canada*

(Received 30 June 2014; revised manuscript received 1 April 2015; published 22 April 2015)

FeF_3, with its half-filled Fe^{3+} $3d$ orbital, hence zero orbital angular momentum and $S = 5/2$, is often put forward as a prototypical highly frustrated classical Heisenberg pyrochlore antiferromagnet. By employing *ab initio* density functional theory, we obtain an effective spin Hamiltonian for this material. This Hamiltonian contains nearest-neighbor antiferromagnetic Heisenberg, biquadratic, and Dzyaloshinskii-Moriya interactions as dominant terms and we use Monte Carlo simulations to investigate the nonzero temperature properties of this minimal model. We find that upon decreasing temperature, the system passes through a Coulomb phase, composed of short-range correlated coplanar states, before transforming into an "all-in/all-out" (AIAO) state via a very weakly first-order transition at a critical temperature $T_c \approx 22$ K, in good agreement with the experimental value for a reasonable set of Coulomb interaction U and Hund's coupling J_H describing the material. Despite the transition being first order, the AIAO order parameter evolves below T_c with a power-law behavior characterized by a pseudo "critical exponent" $\beta \approx 0.18$ in accord with experiment. We comment on the origin of this unusual β value.

DOI: 10.1103/PhysRevB.91.140407 PACS number(s): 75.10.Hk, 71.15.Mb, 75.30.Gw, 75.40.Mg

Systems with magnetic moments on the vertices of two- and three-dimensional networks of corner-shared triangles or tetrahedra and with predominant effective antiferromagnetic nearest-neighbor (n.n.) interactions have tenuous tendency towards conventional long-range magnetic order [1,2]. Consequently, the exotic low-temperature properties of materials with such an architecture are ultimately dictated by the mutual competition of perturbations beyond n.n. interactions [2].

One theoretically expects such highly frustrated magnets to ubiquitously display a *Coulomb phase* (CP) [3]. This is an emergent state with local constraints described by a divergence-free "spin field" and whose defects, where the constraints are violated, behave as effective charges with Coulombic interactions. The CP and its underlying gauge theory description provides an elegant setting to study the effect of various perturbations [4] as well as thermal and quantum fluctuations [5]. A telltale experimental signature of a CP are bow-tie ("pinch points") singularities in the energy-integrated neutron scattering intensity pattern [3,6].

There is good evidence that the classical spin liquid state of spin ice materials with discrete Ising spins may be described by a CP [3,7–9]. Unfortunately, there are few, if any, materials with continuous symmetry spins that display a CP, as may be signaled by pinch points [6]. For example, in $Y_2Mo_2O_7$, complex orbital effects [10,11] and spin glass behavior [12,13] eradicate the CP. In the $ZnCr_2O_4$ spinel, pinch points are not observed [14], likely because perturbations beyond n.n. interactions and spin-lattice coupling eliminate them already at high temperature in the paramagnetic state [4]. In this Rapid Communication we propose that FeF_3, with magnetic Fe^{3+} ions on a pyrochlore network of corner-sharing tetrahedra, may be a strong contender for a CP with Heisenberg spins.

With Fe^{3+} being a $3d$ S-state (spin-only) $S = 5/2$ ion, single-ion anisotropy and anisotropic spin-spin interactions should be small in FeF_3, making it a good candidate material with predominant n.n. Heisenberg exchange. Neutron scattering and Mössbauer experiments find long-range magnetic order below $T_c \approx 20^{+2}_{-5}$ K [15–19]. Yet, the static magnetic susceptibility shows a deviation from the Curie-Weiss law even at 300 K, implying the existence of strong antiferromagnetic exchange and short-range correlations extending up to temperatures much higher than T_c [15] and thus a very high degree of frustration [2,20]. The ordered phase is an "all-in/all-out" (AIAO) state [15] in which the Fe^{3+} magnetic moments point from the corners to the centers (or vice versa) of each tetrahedron [see Fig. 1(a)]. Notably, neutron diffraction experiments find a power-law growth of the AIAO order parameter characterized by a "critical exponent" $\beta \sim 0.18$ [19]. This value differs significantly from standard order-parameter exponents $\beta \sim 1/3$ for three-dimensional systems, which prompted the suggestion of an underlying "new" universality class [19]. There appears to have been no attempt to determine a realistic spin Hamiltonian $\mathcal{H}$ for FeF_3. In this Rapid Communication, we employ density-functional theory (DFT) to flesh out such $\mathcal{H}$ and use it to study the development of correlations upon approaching T_c and to explore the associated critical properties. By computing the energy of various spin configurations and performing Monte Carlo simulations, we expose a highly entropic coplanar (Coulombic) state above T_c and its demise at $T \leqslant T_c$ against an energetically selected AIAO state along with replicating the unusual $\beta \sim 0.18$ exponent.

Spin Hamiltonian and DFT calculations. The classical spin Hamiltonian for FeF_3 is given by

$$\mathcal{H} = \mathcal{H}_{\rm H} + \mathcal{H}_{\rm b.q.} + \mathcal{H}_{\rm r} + \mathcal{H}_{\rm DM} + \mathcal{H}_{\rm s.i.}. \quad (1)$$

*m.alaei@cc.iut.ac.ir
†shahbazi@cc.iut.ac.ir
‡gingras@uwaterloo.ca

 ©2015 American Physical Society

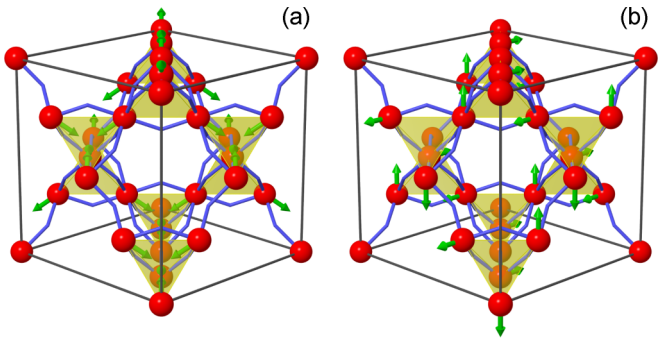

FIG. 1. (Color online) The structure of FeF_3. Red (dark gray) spheres denote the Fe^{3+} ions with their spin indicated by a green arrow. The F^- ions (not shown) are located at the (shown) bends where bonds merge. (a) The AIAO state. (b) A coplanar spin configuration (for clarity, a long-range coplanar state is shown).

$\mathcal{H}_{\rm H} = \sum_{i>j} J_{ij}\, \boldsymbol{S}_i \cdot \boldsymbol{S}_j$ denotes the isotropic Heisenberg term. $\boldsymbol{S}_i$ and $\boldsymbol{S}_j$ are classical unit vectors representing the orientation of the magnetic moments at sites i and j, respectively. We consider a distance-dependent exchange J_{ij} between $\boldsymbol{S}_i$ and $\boldsymbol{S}_j$, with first (J_1), second (J_2), and two distinct third (J_{3a} and J_{3b}) n.n. [21]. $\mathcal{H}_{\rm b.q.} = \sum_{i>j} B_{ij}\,(\boldsymbol{S}_i \cdot \boldsymbol{S}_j)^2$ is the biquadratic interaction with n.n. coupling B_1. $\mathcal{H}_{\rm r} = \sum_{ijkl} K[(\boldsymbol{S}_i \cdot \boldsymbol{S}_j)(\boldsymbol{S}_k \cdot \boldsymbol{S}_l) + (\boldsymbol{S}_j \cdot \boldsymbol{S}_k)(\boldsymbol{S}_l \cdot \boldsymbol{S}_i) - (\boldsymbol{S}_i \cdot \boldsymbol{S}_k)(\boldsymbol{S}_j \cdot \boldsymbol{S}_l)]$ is the ring-exchange interaction. The last two (anisotropic interaction) terms, originating from spin-orbit coupling (SOC), are the Dzyaloshinskii-Moriya (DM) interaction, $\mathcal{H}_{\rm DM} = D \sum_{\langle i,j\rangle} \hat{\mathbf{D}}_{ij} \cdot (\boldsymbol{S}_i \times \boldsymbol{S}_j)$, and single-ion anisotropy $\mathcal{H}_{\rm s.i.} = \Delta \sum_i (\boldsymbol{S}_i \cdot \hat{\mathbf{d}}_i)^2$. $\hat{\mathbf{D}}_{ij}$ are the DM (unit) vectors determined according to the Moriya rules [22,23]. The unit vector $\hat{\mathbf{d}}_i$ denotes the single-ion easy-axis along the local cubic [111] direction at site i.

We next use DFT to study the properties of FeF_3. For all computations, the experimental data for the conventional cubic unit cell lattice parameter (10.325 Å) and position of the ions were used [16]. The DFT calculations were carried out with the full-potential linearized augmented plane wave (FLAPW) method, employing the FLEUR code [31]. We used the local density approximation (LDA) to account for the electron exchange correlation. Electron-electron interactions due to the on-site electron repulsion U are taken into account using the LDA+U method. The effective on-site Coulomb interaction, $U_{\rm eff}$, is defined as $U_{\rm eff} = U - J_{\rm H}$, where U is the bare Coulomb repulsion and $J_{\rm H}$ is the on-site ferromagnetic Hund's exchange, which we set to 1.0 eV, a typical value in such DFT calculations. Using a linear response approach [32], we obtain $U_{\rm eff} \approx 2.8$ eV from the QUANTUM ESPRESSO code [33]. The influence of $U_{\rm eff}$ on various properties is discussed in the Supplemental Material [23]. The minimum energy states possess a global continuous $O(3)$ degeneracy within LDA+U. However, incorporating the effect of SOC within LDA+U+SOC leads to an AIAO configuration with spins along $\langle 111\rangle$ as minimum energy state. We find FeF_3 to be an insulator with a 1.04 eV band gap within LDA+SOC. The band gap rises to 2.49 eV in LDA+U+SOC with $U_{\rm eff} = 2.8$ eV.

We next determine the coupling constants of $\mathcal{H}$ using spin-polarized DFT calculations. For the first three (isotropic) terms of Eq. (1), we use LDA+U to compute the total energy difference between various magnetic configurations [23]. We assume that J_{3b} [21] as well as farther Heisenberg exchanges ($J_m, m \geqslant 4$), and biquadratic terms farther than first n.n. ($B_m, m \geqslant 2$), are negligible. By matching the energy differences for spin-polarized electronic states with that of $\mathcal{H}$, we determine J_1, J_2, J_{3a}, and B_1 [23]. To compute the anisotropic DM (D) and single-ion (Δ) couplings arising from SOC, we use the LDA+U+SOC framework. We consider noncollinear spin-polarized configurations, keeping the isotropic terms of $\mathcal{H}$ unchanged [23]. The largest couplings within LDA+U+SOC are (all in meV)

$$J_1 = 32.7, \quad J_2 = 0.6, \quad J_{3a} = 0.5, \quad B_1 = 1.0, \quad D = 0.6. \qquad (2)$$

The ring exchange K and the single-ion coupling Δ are found to be smaller than 0.1 meV [23], so we henceforth ignore them. The Curie-Weiss temperature, $\theta_{\rm CW}$, can thus be estimated by $\theta_{\rm CW} \sim q J_1/3 \sim 760$ K, where $q = 6$ is the number of n.n. With $\theta_{\rm CW}/T_c \sim 38$, we thus confirm FeF_3 to be a highly frustrated antiferromagnet [2,20].

Ground states and Monte Carlo simulations. Following Refs. [34,35], we find that mean-field theory predicts AIAO order for $\mathcal{H}$ with the above $\{J_1, J_2, J_{3a}, D\}$ values and $B_1 \equiv 0$. This is confirmed by MC simulations when including $B_1 = 1.0$ meV since ($B_1 > 0, D = 0$) stabilizes an $O(3)$ symmetric AIAO state (see discussion below). In the rest of this Rapid Communication, we focus on the *generic* aspects of the collective behavior of the system (such as exponent $\beta \sim 0.18$). While specific details (T_c, and the Fe and F magnetic moments) depend on the value of the ($U, J_{\rm H}$) parameters [23], we expect the overall collective properties to survive small adjustments of these parameters [23]. Therefore, to explore those generic facets, we consider a minimal model Hamiltonian, $\mathcal{H}_{\rm min}$, with $\mathcal{H}_{\rm min} \equiv \mathcal{H}(J_1, B_1, D, J_2 = J_{3a} = 0)$, with the ($J_1, B_1, D$) values of Eq. (2).

The ground state of $\mathcal{H}_{\rm min}$ with ($J_1 > 0, B_1 = D = 0$) is highly degenerate on the pyrochlore lattice [1,35–37]. The ground-state manifold consists of spin configurations with vanishing total spin on each tetrahedron, with two continuous degrees of freedom per tetrahedron [23,35–37]. The minimum energy of $\mathcal{H}_{\rm min}$ with ($J_1 > 0, B_1 > 0, D = 0$) has a globally $O(3)$ degenerate noncoplanar AIAO spin configuration with an angle of 109.47° between each n.n. pair of spins [23]. Including $D > 0$ fixes the spin directions within such a configuration to one of two *discrete* AIAO states with spins along the cubic $\langle 111\rangle$ directions [23]. With $B_1 = 0$, direct DM interactions ($D > 0$) also dictate an AIAO state [22]. The ground-state energy per spin [23] for the coplanar and AIAO state is, respectively, $\epsilon_{\rm coplanar} = -J_1 + B_1 - \sqrt{2}D$ and $\epsilon_{\rm AIAO} = -J_1 + B_1/3 - 2\sqrt{2}D$, showing that the ground state is AIAO *for all* $B_1 > 0$ and $D > 0$ values.

With ($J_1 > 0, B_1 > 0, D = 0$), $\mathcal{H}_{\rm min}$ displays for a tetrahedron three saddle points in its energy landscape which correspond to coplanar states [23]. In these states, two out of four spins are antiparallel along a given axis and perpendicular to the other axis along which the two remaining spins are themselves aligned mutually antiparallel. The addition of

$D > 0$ restricts the orientation of the "coplanes" to be along the xz, xy, or yz planes of the cubic unit cell, depending on which pairs of spins are chosen to be collinear [23]. There are an exponentially large number of such coplanar states which provide an entropy buffer above the critical temperature where the system orders into AIAO. One such coplanar spin arrangement, within the xz plane, is depicted in Fig. 1(b).

We next perform Monte Carlo simulations to gain some insight into the finite-temperature properties of $\mathcal{H}_{\min}$. We use the standard single-spin Metropolis algorithm on lattices consisting of $N = 4 \times L^3$ spins, where L is the linear dimension of the rhombohedral simulation cell. To ensure thermal equilibrium, 10^6 Monte Carlo steps (MCS) per spin were used for each temperature and 10^6 MCS for the data collection. To reduce the correlation between measurements, 10 to 20 MC sweeps were discarded between successive data collection. To ascertain that our results are fully thermally equilibrated and are not caused by a two-phase coexistence, we started the simulation runs from different initial states, i.e., totally disordered, AIAO ordered, and coplanar states, and checked that all final results remain the same.

Quantities of particular interest are the AIAO order parameter $m \equiv \Sigma_{i,a} \boldsymbol{S}_i^a \cdot \hat{\mathbf{d}}^a / N$ ($\hat{\mathbf{d}}^a$ is the local cubic [111] direction for sublattice a) and the Binder fourth-order cumulant for both m and energy E, defined respectively as $U_m(T) \equiv 1 - \frac{1}{3}\frac{\langle m^4 \rangle}{\langle m^2 \rangle^2}$ and $U_E(T) \equiv 1 - \frac{1}{3}\frac{\langle E^4 \rangle}{\langle E^2 \rangle^2}$. U_m vanishes in the paramagnetic phase, with a Gaussian probability distribution for m, while U_m approaches $2/3$ in the ordered phase [38–40]. U_E tends asymptotically to $2/3$ in both the ordered and paramagnetic phase while reaching a minimum, $U_E^{\min}$, near the transition [23].

The temperature dependence of m and U_m is shown in the main panel and top inset of Fig. 2. Both plots indicate a narrow critical region around $T \approx 0.06$. The left inset in Fig. 2 shows the finite-size scaling of m for different L according to the finite-size scaling behavior $m = L^{-\beta/\nu}\mathcal{M}(tL^{1/\nu})$. Here $t \equiv (T_c - T)/T_c$ is the reduced temperature, β is the order parameter exponent, ν is the correlation length exponent, and $\mathcal{M}$ is the scaling function [40]. This analysis yields $T_c/J_1 = 0.0601(2)$, $\beta = 0.18(2)$, and $\nu = 0.60(2)$. With $J_1 = 32.7$ meV $=$ 379.47 K, we get $T_c \approx 22$ K, in good agreement with the experimental value [15–17,19]. Perhaps most noteworthy, the Monte Carlo exponent $\beta \approx 0.18$ value corresponds to that found in experiment [19]. While these scaling arguments naively suggest that the transition is second order, it is instructive to consider the L dependence of $U_E^{\min}$ which, for a first-order transition, is given by [40], $U_E^{\min}(L) = U^* + AL^{-d} + O(L^{-2d})$, with $U^* < 2/3$. Here $d = 3$ is the space dimension and A is a constant. The precise linear fit of $U_E^{\min}(L)$ versus L^{-3}, with $U^* = 0.666664(1)$, hence very close to $2/3$, that we find (see Fig. 10 in the Supplemental Material [23]) suggests that the transition might actually be very weakly first order.

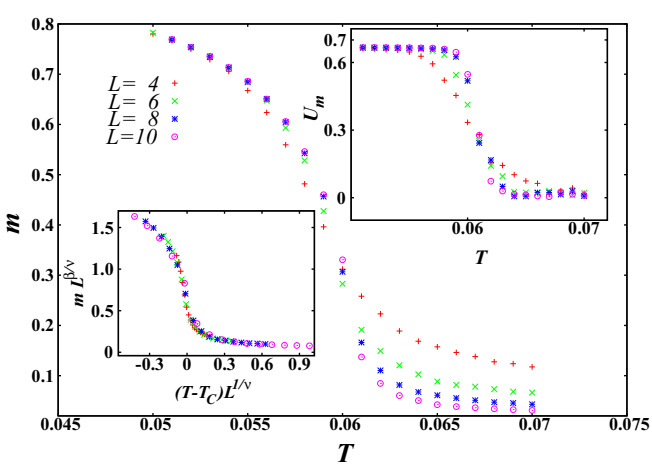

FIG. 2. (Color online) Main panel: Variation of the AIAO order parameter (m) versus temperature (in units of J_1), for lattices of linear size $L = 4,6,8,10$. Top inset: Fourth-order Binder cumulant of m versus temperature, T (in units of J_1), for the same lattice sizes. Left inset: Finite-size scaling of $m(t,L)$ with $\beta = 0.18(2)$ and $\nu = 0.60(2)$.

To shed further light on the nature of the transition, we compute the probability distribution function of the order parameter per tetrahedron, $P(m_n)$, with $m_n \equiv \Sigma_{a=1}^4 \boldsymbol{S}^a \cdot \hat{\mathbf{d}}^a$. We also compute the probability distribution function of two distinct four-spin correlations within each tetrahedron, $P(R)$ and $P(\tilde{R})$, with

$$R \equiv (\boldsymbol{S}_1 \cdot \boldsymbol{S}_2)(\boldsymbol{S}_3 \cdot \boldsymbol{S}_4) + (\boldsymbol{S}_1 \cdot \boldsymbol{S}_3)(\boldsymbol{S}_2 \cdot \boldsymbol{S}_4) + (\boldsymbol{S}_1 \cdot \boldsymbol{S}_4)(\boldsymbol{S}_2 \cdot \boldsymbol{S}_3),$$

$$\tilde{R} \equiv |(\boldsymbol{S}_1 \cdot \boldsymbol{S}_2)(\boldsymbol{S}_3 \cdot \boldsymbol{S}_4) - (\boldsymbol{S}_1 \cdot \boldsymbol{S}_3)(\boldsymbol{S}_2 \cdot \boldsymbol{S}_4) + (\boldsymbol{S}_1 \cdot \boldsymbol{S}_4)(\boldsymbol{S}_2 \cdot \boldsymbol{S}_3)|.$$

Figures 3(a)–3(c) show $P(m_n)$, $P(R)$, and $P(\tilde{R})$ versus T for $L = 10$. $P(m_n)$ is a Gaussian centered at $m_n = 0$ for $T \gg T_c$. As T decreases, $P(m_n)$ deviates from a Gaussian near T_c, developing *four* peaks with $m_n \neq 0$ for $T \lesssim T_c$. Well below the transition, only two peaks at $|m_n| \approx 4$ remain, corresponding to almost perfect AIAO order. The peculiar temperature evolution of $P(m_n)$ suggests that another state coexists or competes with the AIAO state near T_c. The nature of this other state can be clarified by considering $P(R)$ and $P(\tilde{R})$ in Figs. 3(b) and 3(c), respectively. Two peaks arise in $P(R)$ at $T \gtrsim T_c$: one at $R \approx 1/3$ and another at $R \approx 1$ [see Fig. 3(b)]. The former corresponds to an AIAO spin configuration for which $(\boldsymbol{S}_a \cdot \boldsymbol{S}_b) = -\frac{1}{3}$ at $T \ll J_1$ for two n.n. spins. The peak at $R = 1$ is consistent with coplanar states as deduced from Eq. (3). Considering $P(\tilde{R})$ in Fig. 3(c), one observes a peak at $\tilde{R} \approx 1$ near T_c. One can easily show [23] that the two equations for $R = 1/3$ and $\tilde{R} = 1$ have *no common* solution for a zero net spin/moment on a tetrahedron. Therefore, an AIAO state does not produce the peak at $\tilde{R} \approx 1$, which must therefore originate from the competing state. One can show that Eqs. (3) for $R = 1$ and $\tilde{R} = 1$ admit three solutions [23], which are precisely the xy, xz, and yz coplanar states discussed above. The "competing state" at $T \gtrsim T_c$ is therefore short-range coplanar, is divergence-free in the "spin field," and should thus be viewed as a CP [3]. To expose further the CP nature of the state at $T \gtrsim T_c$, we compute the neutron structure factor $S(\boldsymbol{q})$ (second row of Fig. 3) in the (hhl) scattering plane as a function of T. At $T = 0.1$, clear pinch points (marked by arrows) are visible. Some of these pinch points (solid arrows) turn into magnetic Bragg preaks ($T \sim 0.06$) while others (dashed arrows) become mere weak diffuse spots (forbidden Bragg peaks [23]) upon going through the transition to AIAO order

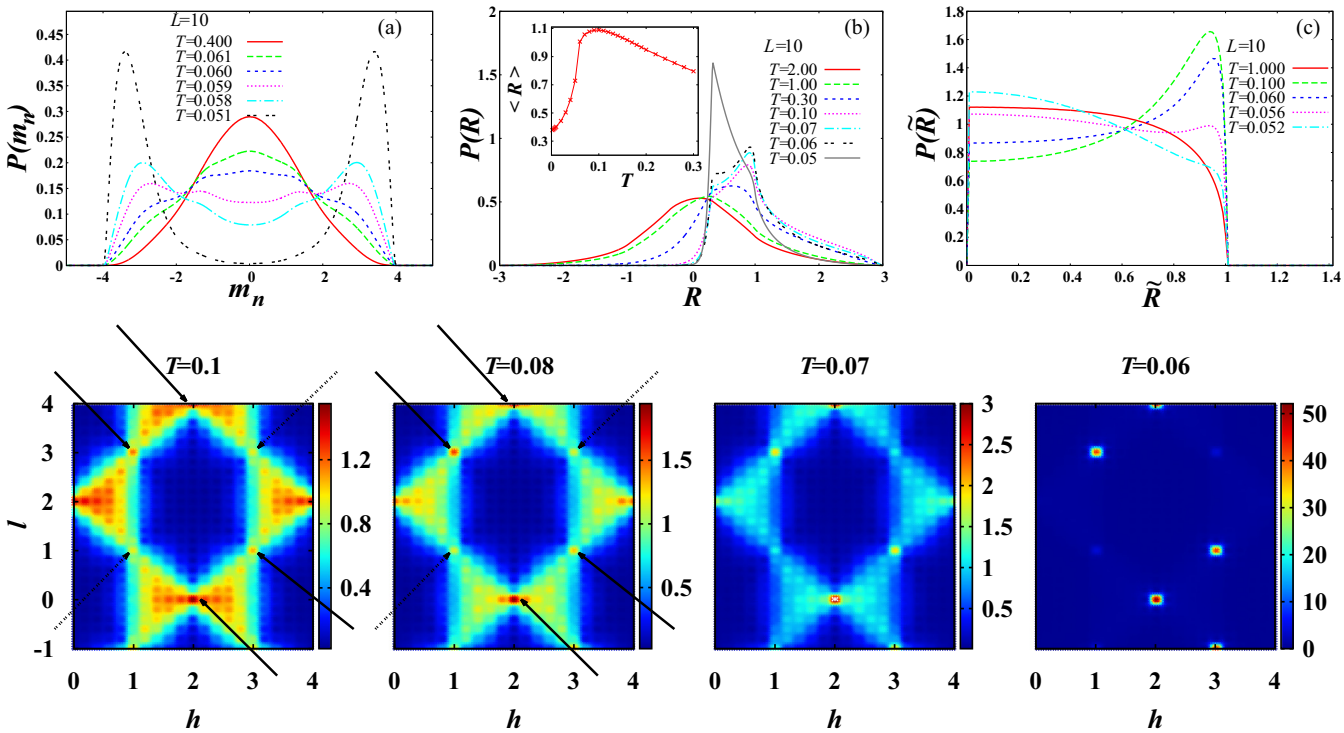

FIG. 3. (Color online) Top row: Probability distribution functions, $P(m_n)$, $P(R)$, and $P(\tilde{R})$, as a function of temperature T and for a lattice of linear size $L = 10$. The inset of panel (b) shows the T dependence of $\langle R \rangle$, which displays a sharp drop at $T_c \approx 0.06$, a further indication for the discontinuous nature of the transition. Bottom row: Temperature evolution of the neutron structure factor, $S(\boldsymbol{q})$, in the (hhl) plane as T approaches T_c from the paramagnetic phase. The arrows indicate the location of pinch points for the $T = 0.1$ and $T = 0.08$ panels (see text).

at T_c (see $T = 0.08$, $T = 0.07$, and $T = 0.06$ panels in bottom row of Fig. 3).

Conclusion. Using DFT, we determined the predominant couplings of the spin Hamiltonian of the FeF_3 pyrochlore Heisenberg antiferromagnet. We find that biquadratic exchange and anisotropic direct Dzyaloshinskii-Moriya interactions conspire to select an all-in/all-out ground state. Monte Carlo simulations find a transition to that state at a critical temperature $T_c \approx 22$ K, in good agreement with experiments. The transition is characterized by an order parameter pseudo "critical exponent" $\beta \approx 0.18$, that is also in agreement with experiment. We view this exponent not as signaling an unusual universality class, but rather as an effective power-law parametrization near a very weakly first-order transition, perhaps near a mean-field tricritical point for which $\beta = 1/4$ (up to logarithmic correction because three dimensions is the upper critical dimension for tricritical behavior [41]). Indeed, for $D/J_1 \lesssim 0.01$, the transition is found to be strongly first order while it is second order and in the three-dimensional Ising universality class for $D/J_1 \gtrsim 0.1$ [42]. We find the state above T_c to be composed of entropically favored coplanar states without long-range magnetic order and thus a Coulomb phase [3]. We hope that our study will motivate a new generation of experiments on FeF_3, perhaps even on single-crystal samples, which we would anticipate on the basis of our work to display interesting properties heretofore unexposed in highly frustrated Heisenberg pyrochlore antiferromagnets.

Acknowledgments. We thank Bob Cava, Peter Holdsworth, Takashi Imai, Hikaru Kawamura, Seunghun Lee, Paul McClarty, Nic Shannon, Oleg Tchernyshyov, and Anson Wong for useful discussions. We acknowledge Hojjat Gholizadeh for help with the pyrochlore lattice figures. This work was made possible by the facilities of the Shared Hierarchical Academic Research Computing Network (SHARCNET; https://www.sharcnet.ca) and Compute/Calcul Canada. One of us (M.G.) thanks Harald Jeschke for most useful discussions regarding DFT calculations for magnetic systems. M.G. acknowledges support from the Canada Council for the Arts and the Perimeter Institute for Theoretical Physics. Research at PI is supported by the Government of Canada through Industry Canada and by the Province of Ontario through the Ministry of Economic Development and Innovation.

[1] J. Villain, Z. Phys. B **33**, 31 (1979).
[2] C. Lacroix, P. Mendels, and F. Mila, *Introduction to Frustrated Magnetism*, Springer Series in Solid-State Sciences (Springer, Heidelberg, 2011).
[3] C. L. Henley, Annu. Rev. Condens. Matter Phys. **1**, 179 (2010).
[4] P. H. Conlon and J. T. Chalker, Phys. Rev. B **81**, 224413 (2010).
[5] M. J. P. Gingras and P. A. McClarty, Rep. Prog. Phys. **77**, 056501 (2014).
[6] M. P. Zinkin, M. J. Harris, and T. Zeiske, Phys. Rev. B **56**, 11786 (1997).
[7] C. Castelnovo, R. Moessner, and S. L. Sondhi, Annu. Rev. Condens. Matter Phys. **3**, 35 (2012).

[8] T. Fennell, P. P. Deen, A. R. Wildes, K. Schmalzl, D. Prabhakaran, A. T. Boothroyd, R. J. Aldus, D. F. Mcmorrow, and S. T. Bramwell, Science **326**, 415 (2009).

[9] D. J. P. Morris, D. A. Tennant, S. A. Grigera, B. Klemke, C. Castelnovo, R. Moessner, C. Czternasty, M. Meissner, K. C. Rule, J.-U. Hoffmann, K. Kiefer, S. Gerischer, D. Slobinsky, and R. S. Perry, Science **326**, 411 (2009).

[10] H. Shinaoka, Y. Motome, T. Miyake, and S. Ishibashi, Phys. Rev. B **88**, 174422 (2013).

[11] H. J. Silverstein, K. Fritsch, F. Flicker, A. M. Hallas, J. S. Gardner, Y. Qiu, G. Ehlers, A. T. Savici, Z. Yamani, K. A. Ross, B. D. Gaulin, M. J. P. Gingras, J. A. M. Paddison, K. Foyevtsova, R. Valenti, F. Hawthorne, C. R. Wiebe, and H. D. Zhou, Phys. Rev. B **89**, 054433 (2014).

[12] M. J. P. Gingras, C. V. Stager, N. P. Raju, B. D. Gaulin, and J. E. Greedan, Phys. Rev. Lett. **78**, 947 (1997).

[13] J. S. Gardner, B. D. Gaulin, S.-H. Lee, C. Broholm, N. P. Raju, and J. E. Greedan, Phys. Rev. Lett. **83**, 211 (1999).

[14] S.-H. Lee, C. Broholm, W. Ratcliff, G. Gasparovic, Q. Huang, T. H. Kim, and S.-W. Cheong, Nature (London) **418**, 856 (2002).

[15] M. Leblanc, J. Pannetier, G. Ferey, and R. Depape, Rev. Chim. Miner. **22**, 107 (1985).

[16] R. De Pape and G. Ferey, Mater. Res. Bull. **21**, 971 (1986).

[17] Y. Calage, M. Zemirli, J. M. Greneche, F. Varret, R. De Pape, and G. Ferey, J. Solid State Chem. **69**, 197 (1987).

[18] J. N. Reimers, J. E. Greedan, C. V. Stager, M. Bjorgvinnsen, and M. A. Subramanian, Phys. Rev. B **43**, 5692 (1991).

[19] J. N. Reimers, J. E. Greedan, and M. Björgvinsson, Phys. Rev. B **45**, 7295 (1992).

[20] A. P. Ramirez, Annu. Rev. Mater. Sci. **24**, 453 (1994).

[21] There are two types of third-nearest neighbors, one with two Fe-F-Fe bonds, with exchange J_{3a}, and the other with three Fe-F-Fe bonds with exchange J_{3b}, in between (see Fig. 1 in the Supplemental Material [23]). In the strong-coupling perturbation theory, addition of each intermediate ion increases the order of perturbation and makes the resulting superexchange interaction smaller.

[22] M. Elhajal, B. Canals, R. Sunyer, and C. Lacroix, Phys. Rev. B **71**, 094420 (2005).

[23] See Supplemental Material at http://link.aps.org/supplemental/10.1103/PhysRevB.91.140407 for details pertaining to the DTFT calculations, the properties of the energy landscape due to the bi-quadratic interactions, definition of the DM vectors and additional Monte Carlo results providing further evidence for short-range coplanar states above T_c. The Supplemental Material includes additional references [24–30].

[24] J. Owen and J. H. M. Thornley, Rep. Prog. Phys. **29**, 675 (1966).

[25] A. G. Del Maestro and M. J. P. Gingras, J. Phys.: Condens. Matter **16**, 3339 (2004); Phys. Rev. B **76**, 064418 (2007).

[26] J. B. Forsyth, P. J. Brown, and B. M. Wanklyn, J. Phys. C: Solid State Phys. **21**, 2917 (1988).

[27] J. P. Perdew, K. Burke, and M. Ernzerhof, Phys. Rev. Lett. **77**, 3865 (1996).

[28] E. Bousquet and N. Spaldin, Phys. Rev. B **82**, 220402(R) (2010).

[29] T. Moriya, Phys. Rev. **120**, 91 (1960).

[30] N. Shannon, K. Penc, and Y. Motome, Phys. Rev. B **81**, 184409 (2010).

[31] See http://www.flapw.de.

[32] M. Cococcioni and S. de Gironcoli, Phys. Rev. B **71**, 035105 (2005).

[33] P. Giannozzi, S. Baroni, N. Bonini, M. Calandra, R. Car, C. Cavazzoni, D. Ceresoli, G. L. Chiarotti, M. Cococcioni, I. Dabo, A. Dal Corso, S. Fabris, G. Fratesi, S. de Gironcoli, R. Gebauer, U. Gerstmann, C. Gougoussis, A. Kokalj, M. Lazzeri, L. Martin-Samos, N. Marzari, F. Mauri, R. Mazzarello, S. Paolini, A. Pasquarello, L. Paulatto, C. Sbraccia, S. Scandolo, G. Sclauzero, A. P. Seitsonen, A. Smogunov, P. Umari, and R. M. Wentzcovitch, J. Phys.: Condens. Matter **21**, 395502 (2009).

[34] M. Enjalran and M. J. P. Gingras, Phys. Rev. B **70**, 174426 (2004).

[35] J. N. Reimers, A. J. Berlinsky, and A.-C. Shi, Phys. Rev. B **43**, 865 (1991).

[36] R. Moessner and J. T. Chalker, Phys. Rev. Lett. **80**, 2929 (1998).

[37] R. Moessner and J. T. Chalker, Phys. Rev. B **58**, 12049 (1998).

[38] K. Binder, J. Comput. Phys. **59**, 1 (1985).

[39] M. S. S. Challa, D. P. Landau, and K. Binder, Phys. Rev. B **34**, 1841 (1986).

[40] D. P. Landau and K. Binder, *A Guide to Monte Carlo Simulations in Statistical Physics* (Cambridge University Press, Cambridge, 2000).

[41] M. J. Stephen, E. Abrahams, and J. P. Straley, Phys. Rev. B **12**, 256 (1975).

[42] We found similar behavior in a toy model with solely $J_1 = 1$ and $\Delta < 0$, and so did others (P. C. W. Holdsworth, unpublished; H. Kawamura, unpublished).